Synthesis and Structural Characterization of Compounds Containing the $[Zr_6Cl_{18}H_5]^{3-}$ Cluster Anion. Determination of the Number of Cluster Hydrogen Atoms

Linfeng Chen, F. Albert Cotton,* and William A. Wojtczak

Department of Chemistry and Laboratory for Molecular Structure and Bonding, Texas A&M University, College Station, Texas 77843

Received February 16, 1996[⊗]

Reduction of $ZrCl_4$ with $HSnBu_3$ followed by addition of $[R_4A]Cl$ resulted in the formation of $[R_4A]_3[Zr_6Cl_{18}H_5]$ (**2a**, R = Ph, A = P; **2b**, R = *n*-Pr, A = N; **2c**, R = Et, A = N). Six zirconium atoms are arranged as an octahedron with one Cl atom terminally coordinated to each Zr atom and the other 12 Cl atoms edge-bridging the octahedron. When $[Ph_4P]I$ was used, the compound $[Ph_4P]_3[Zr_6Cl_{18-x}I_xH_5]$ (x = 0.81) (**3**) was isolated. In compound **3**, I atoms occupy only the terminal positions. The number of cluster hydrogen atoms in compounds **2a**−**c** and **3** was established by ^{1}H NMR. The X-ray results are consistent with the five cluster hydrogen atoms being distributed at or slightly outside the centers of all eight triangular faces of the octahedron. Compounds **2a**−**c** and **3** were characterized by X-ray single-crystal diffraction. Compound **2a**·$3CH_2Cl_2$ crystallized in the triclinic space group $P\bar{1}$ with cell dimensions (20 °C) of a = 15.993(3) Å, b = 22.237(3) Å, c = 14.670(4) Å, α = 95.31(1)°, β = 112.07(2)°, γ = 82.06(2)°, V = 4784(2) Å^3, and Z = 2. Compound **2a** crystallized in the tetragonal space group $I4_1/a$ with cell dimensions (20 °C) of a = 33.196(2) Å, b = 33.196(2) Å, c = 15.236(2) Å, V = 16790(3) Å^3, and Z = 8. Compound **2a**·$4C_6H_5CH_3$ crystallized in the triclinic space group $P\bar{1}$ with cell dimensions (−60 °C) of a = 14.501(5) Å, b = 26.630(9) Å, c = 14.049(5) Å, α = 90.39(3)°, β = 94.19(3)°, γ = 82.59(1)°, V = 5365(3) Å^3, and Z = 2. Compound **2b** crystallized in the cubic space group $Im\bar{3}m$ with cell dimensions (−60 °C) of a = 15.039(3) Å, b = 15.039(3) Å, c = 15.039(3) Å, V = 3438(1) Å^3, and Z = 2. Compound **2c**·2.43MeCN crystallized in the orthorhombic space group *Pnma* with cell dimensions (−100 °C) of a = 21.156(1) Å, b = 24.584(3) Å, c = 11.713(2) Å, V = 6092(1) Å^3, and Z = 4. Compound **3**·$3CH_2Cl_2$·$C_6H_5CH_3$ crystallized in the monoclinic space group $P2_1/c$ with cell dimensions (20 °C) of a = 19.786(5) Å, b = 19.071(4) Å, c = 27.397(5) Å, β = 90.22(3)°, V = 10337(4) Å^3, and Z = 4.

Introduction

A series of octahedral $Zr_6X_{12}Z$ (X = Cl, Br, I) type compounds have been synthesized through high-temperature solid-state reactions.[1] In these compounds, an atom of either a non-metal (Be, B, C, N)[2] or a metal (Fe, Co, Ni)[3,4] occupies the center of the cluster. It was believed that the central atom and the electrons it could contribute to the bonding of the Zr_6 cluster were essential to the stabilization of the cluster.[4] Two Zr_6 compounds containing a cluster hydrogen atom (or atoms), $Zr_6Cl_{12}H$[5] and $Li_6[Zr_6Cl_{18}H]$,[6] were also obtained from solid state synthesis. Displacement of chlorides in $Li_6Zr_6Cl_{18}H$ by $EtNH_2$ resulted in the formation of another hydrogen-containing cluster compound, $Zr_6Cl_{12}H(EtNH_2)_6$.[7] In the effort to characterize the interstitial hydrogen, $Li_6[Zr_6Cl_{18}H]$ was studied by inelastic neutron scattering, and the observations were rationalized in terms of a model with the hydrogen occupying a μ^3-bridging position within the octahedral interstitial site with a Zr−H bond distance of *ca.* 2.0 Å.[8] $Zr_6Cl_{12}H$ was studied by solid-state NMR.[5] The results indicated that the hydridic species undergoes random motion on the NMR time scale, in accord with the oversized Zr_6 metal cluster cavity available. However, the number and positions of the cluster hydrogen atoms have never been unambiguously determined.

By reducing ZrX_4 (X = Cl, Br) with $HSnBu_3$, we have developed a new method to prepare zirconium cluster compounds containing cluster hydrogen atoms under mild reaction conditions (room temperature in organic solvents).[9−12] The reduction of $ZrCl_4$ with $HSnBu_3$ followed by addition of phosphines yielded pentanuclear cluster compounds $[Zr_5Cl_{12}(PR_3)_5H_4]$ and three types of hexanuclear cluster species, principally $[Zr_6Cl_{14}(PR_3)_4H_4]$ and $[Zr_6Cl_{18}H_5]^{3-}$, but also small amounts of $[Zr_6Cl_{18}H_4]^{4-}$.[12] In the pyramidal pentanuclear compounds, $[Zr_5Cl_{12}(PR_3)_5H_4]$, two cluster hydrogen atoms are μ_3-bridging two opposite triangular faces and the other two are μ_2-bridging two opposite basal edges.[10] In the octahedral hexanuclear compounds, $[Zr_6Cl_{14}(PR_3)_4H_4]$, four cluster hydrogen atoms were detected and appear to be distributed over the

[⊗] Abstract published in *Advance ACS Abstracts,* August 1, 1997.

(1) For recent reviews see: (a) Corbett, J. D.; Garcia, E.; Kwon, Y.-U.; Guloy, A. *High Temp. Sci.* **1990**, *27*, 337. (b) Rogel, F.; Zhang, J.; Payne, M. W.; Corbett, J. D. *Adv. Chem. Ser.* **1990**, *226*, 369. (c) Corbett, J. D.; Ziebarth, R. P. *Acc. Chem. Res.* **1989**, *22*, 256.
(2) (a) Ziebarth, R. P.; Corbett, J. D. *J. Solid State Chem.* **1989**, *80*, 56. (b) Smith, J. D.; Corbett, J. D. *J. Am. Chem. Soc.* **1985**, *107*, 5704. (c) Zhang, J.; Corbett, J. D. Z. *Anorg. Allg. Chem.* **1991**, *598*, 363.
(3) Hughbanks, T.; Rosenthal, G.; Corbett, J. D. *J. Am. Chem. Soc.* **1986**, *108*, 8289.
(4) Hughbanks, T.; Rosenthal, G.; Corbett, J. D. *J. Am. Chem. Soc.* **1988**, *110*, 1511.
(5) Chu, P. J.; Ziebarth, R. P.; Corbett, J. D.; Gerstein, B. C. *J. Am. Chem. Soc.* **1988**, *110*, 5324.
(6) Hart, D. W.; Teller, R. G.; Wei, C. Y.; Bau, R.; Longoni, G.; Campanella, S.; Chini, P.; Koetzle, T. F. *Angew. Chem., Int. Ed. Engl.* **1979**, *18*, 80; *J. Am. Chem. Soc.* **1981**, *103*, 1458.
(7) Rogel, F.; Corbett, J. D. *J. Am. Chem. Soc.* **1990**, *112*, 8189.
(8) Corbett, J. D.; Eckert, J.; Jayasooriya, U. A.; Kearley, G. J.; White, R. P.; Zhang, J. *J. Phys. Chem.* **1993**, *97*, 8384.
(9) Chen, L.; Cotton, F. A.; Wojtczak, W. A. *Angew. Chem., Int. Ed. Engl.* **1995**, *34*, 1877.
(10) Cotton, F. A.; Lu, J.; Shang, M.; Wojtczak, W. A. *J. Am. Chem. Soc.* **1994**, *116*, 4364.
(11) (a) Cotton, F. A.; Feng, X.; Shang, M.; Wojtczak, W. A. *Angew. Chem., Int. Ed. Engl.* **1992**, *31*, 1050. (b) Chen, L.; Cotton, F. A.; Wojtczak, W. A. *Inorg. Chem.* **1996**, *35*, 2988.
(12) Chen, L.; Cotton, F. A.;Wojtczak, W. A. *Inorg. Chim. Acta* **1996**, *252*, 239.

S0020-1669(96)00173-5 CCC: $14.00

eight triangular faces of the octahedron, near the centers of the Zr_3 triangles.[12]

Compounds containing the $[Zr_6Cl_{18}H_5]^{3-}$ cluster anion can be directly prepared in a similar way. Reaction of $ZrCl_4$ with $HSnBu_3$ followed by addition of $[R_4A]Cl$ allowed the isolation of $[Ph_4P]_3[Zr_6Cl_{18}H_5]$ (**2a**), $[Pr_4N]_3[Zr_6Cl_{18}H_5]$ (**2b**), and $[Et_4N]_3[Zr_6Cl_{18}H_5]$ (**2c**). When $[Ph_4P]I$ was used, compound $[Ph_4P]_3[Zr_6Cl_{18-x}I_xH_5]$ (**3**) was obtained. Now we wish to report the details of the synthesis and characterization of compounds **2a**−**c** and **3**. A preliminary report of a portion of this work has been published.[9]

Experimental Section

All manipulations were conducted under an argon atmosphere by using standard vacuum-line and Schlenk techniques. Glassware was oven-dried at 150 °C for 24 h prior to use. Solvents were predried over molecular sieves and freshly distilled under nitrogen from appropriate drying reagents. $ZrCl_4$, $[Ph_4P]Cl$, $[Ph_4P]I$, $[Pr_4N]Cl$, $[Et_4N]Cl$, and $[Et_4N]CN$ were purchased from Strem Chemicals and dried at 150 °C under vacuum for 24 h. $HSnBu_3$ and $DSnBu_3$ were purchased from Aldrich and used as received. ^1H and ^2H NMR spectra were recorded on a Varian XL-200E and a XL-200 broad band spectrometer, respectively.

Reduction of $ZrCl_4$ with $HSnBu_3$. $ZrCl_4$ (466 mg, 2.0 mmol) was reduced with $HSnBu_3$ (1.15 mL, 4.0 mmol) in 20 mL of toluene with vigorous stirring for 30 h. The orange supernatant liquid was decanted. The solid was washed with two portion of fresh toluene to give the brown solid **1**.

Preparation of $[Ph_4P]_3[Zr_6Cl_{18}H_5]$, 2a. A 375 mg (1.0 mmol) sample of $[Ph_4P]Cl$ in 15 mL of CH_2Cl_2 was added to the brown solid **1**. The brown solid was immediately solubilized, producing a purple solution. The purple solution was transferred to a Schlenk tube and layered with 30 mL of hexane. *Ca*. 190 mg (23%) of rhomboidal dark purple crystals of **2a**·$3CH_2Cl_2$ was isolated in 2 weeks after the diffusion was completed. In order to make an accurate comparison of the integrated intensities, a single-crystal of **2a**·$3CH_2Cl_2$ having a size of *ca*. 3.0 mm × 3.0 mm × 3.0 mm was used for ^1H NMR measurements. ^1H NMR for **2a**·$3CH_2Cl_2$ (δ in CD_3CN, ppm): 7.88 (m, C_6H_5, 12H), 7.71 (m, C_6H_5, 48H), −3.07 (s, Zr_6H_5, 5H, $\Delta\nu_{1/2}$ = 1.83 Hz at 20 °C). Another crystalline form of compound **2a**, *ca*. 2% (15 mg), was also isolated at the initial position of the interface between CH_2Cl_2 and hexane as large, thin, platelike dark purple crystals. The composition was determined by X-ray single-crystal diffraction as **2a**·$4C_6H_5CH_3$. The ^1H NMR spectrum indicated that it contained the same cluster anion, $[Zr_6Cl_{18}H_5]^{3-}$. In addition, *ca*. 460 mg (20% yield) of colorless crystals of $[Ph_4P]_2[ZrCl_6]$·$2CH_2Cl_2$ (a = 11.152(3) Å, b = 12.435(5) Å, c = 10.240(5) Å, α = 90.27(3)°, β = 99.61(7)°, γ = 70.83(3)°) was obtained.[13]

When the reaction was carried out in CH_3CN and the resulting purple solution was layered with 2 mL of hexane and then 30 mL of Et_2O, another crystalline form of compound **2a** was isolated in a yield of *ca*.15% in 3 weeks. Results from X-ray single-crystal diffraction showed there are no solvent molecules. The composition of $[Ph_4P]_3[Zr_6Cl_{18}H_5]$ was also confirmed by an ^1H NMR study. The unreduced $ZrCl_4$ was isolated as $[Ph_4P]_2[ZrCl_6]$·$4CH_3CN$ (*ca*. 440 mg, 18% yield).[14]

Preparation of $[Ph_4P]_3[Zr_6Cl_{18}D_5]$, 2a*. $[Ph_4P]_3[Zr_6Cl_{18}D_5]$, **2a***, was prepared in the same manner as described for **2a**·$3CH_2Cl_2$ by using $DSnBu_3$ instead of $HSnBu_3$. The ^1H NMR spectrum showed signals for $[Ph_4P]^+$ and a very weak signal at −3.07 ppm, which was due to incomplete deuteration of the $DSnBu_3$ reagent (97 % D).

Preparation of $[Ph_4P]_3[Zr_6Cl_{18}(H_{1/2}D_{1/2})_5]$, 2a.** $[Ph_4P]_3[Zr_6Cl_{18}(H_{1/2}D_{1/2})_5]$, **2a****, was also prepared in the manner described above for **2a**·$3CH_2Cl_2$ by using a reducing reagent comprising 50% $DSnBu_3$ and 50% $HSnBu_3$ instead of pure $HSnBu_3$. The ^1H NMR spectrum of $[Zr_6Cl_{18}(H_{1/2}D_{1/2})_5]^{3-}$ showed a signal at −3.07 ppm that is broader, $\Delta\nu_{1/2}$(20 °C) = 3.12 Hz, than that in the spectrum of $[Zr_6Cl_{18}H_5]^{3-}$, $\Delta\nu_{1/2}$(20 °C) = 1.83 Hz. However, no resolved H−D coupling was observed. Conversely, the ^2H NMR spectrum of $[Zr_6Cl_{18}(H_{1/2}D_{1/2})_5]^{3-}$, showing a signal at −3.00 ppm ($CDHCl_2$ as reference in CH_2Cl_2), had a broader ^2H signal, 2.7 Hz, when recorded without H-decoupling than that observed, 2.2 Hz, when the spectrum was recorded with ^1H decoupling. Again, no resolved coupling between the D atom and the H atom was observed.

Reaction of 1 with CH_3CN. A 15 mL portion of CH_3CN was added to the brown solid **1** to produce a dark purple solution. This purple solution was transferred to a Schlenk tube and layered with 2 mL of hexane and then 30 mL of Et_2O. No crystal was obtained, and the purple color vanished in 12 h.

The decomposition process was monitored by ^1H NMR. The brown solid **1** was dissolved in CD_3CN to give a purple solution. The cluster anion, $[Zr_6Cl_{18}H_5]^{3-}$, was detected at the beginning, along with signals from butyl groups. The cluster anion was decomposed completely within 12 h.

Preparation of $[Pr_4N]_3[Zr_6Cl_{18}H_5]$, 2b. The preparation of $[Pr_4N]_3[Zr_6Cl_{18}H_5]$, **2b**, was carried out in a fashion similar to that described above for compound **2a** by using $[Pr_4N]Cl$ instead of $[Ph_4P]Cl$. The crystalline yield was *ca*. 15% (86 mg). ^1H NMR (δ in CH_3CN, ppm): 3.03 (m, $CH_2CH_2CH_3$, 24H), 1.61 (m, $CH_2CH_2CH_3$, 24H), 0.92 (t, $^3J_{H-H}$ = 7 Hz, $CH_2CH_2CH_3$, 36H), −3.07 (s, Zr_6H_5, 5H).

Preparation of $[Et_4N]_3[Zr_6Cl_{18}H_5]$, 2c. (1) $[Et_4N]_3[Zr_6Cl_{18}H_5]$, **2c**, was prepared in a manner similar to that described above for compound **2a** by using $[Et_4N]Cl$ instead of $[Ph_4P]Cl$. *Ca*. 112 mg (20% yield) of dark purple crystals of **2c**·$2.43CH_3CN$ was isolated. ^1H NMR (δ in CH_3CN, ppm): 3.18 (q, $^3J_{H-H}$ = 7 Hz, CH_2CH_3, 24H), 1.21 (t, $^3J_{H-H}$ = 7 Hz, CH_2CH_3, 36H), −3.07 (s, Zr_6H_5, 5H).

(2) After the brown solid **1** was dissolved in 15 mL of CH_3CN, 268 mg (1.0 mmol) of $[Et_4N]_4CN$ was added to the solution. The solution was transferred to a Schlenk tube and layered with 2 mL of hexane and then 30 mL of Et_2O. *Ca*. 78 mg (14%) of crystalline **2c**·$2.43CH_3CN$ was isolated.

Preparation of $[Ph_4P]_3[Zr_6Cl_{18-x}I_xH_5]$, 3. $[Ph_4P]_3[Zr_6Cl_{18-x}I_xH_5]$, **3**, was prepared in a manner similar to that described above for compound **2a**·$3CH_2Cl_2$ by using $[Ph_4P]I$ instead of $[Ph_4P]Cl$. It was isolated as dark purple crystals of $[Ph_4P]_3[Zr_6Cl_{18-x}I_xH_5]$·$3CH_2Cl_2$·$C_6H_5CH_3$ in *ca*. 18% yield (158 mg). The composition of **3** was $[Ph_4P]_3[Zr_6Cl_{18-x}I_xH_5]$ with x = 2.4 from the refinement results of X-ray single-crystal diffraction data when compound **3** was first crystallized from the solution. After recrystallization, the value of x decreased to 0.81. ^1H NMR for compound **3** with x = 0.81 (δ in CH_3CN, ppm): 7.88 (m, C_6H_5, 12H), 7.71 (m, C_6H_5, 48H), −3.07 (s, Zr_6H_5, 5H, broad, $\Delta\nu_{1/2}$ = 6.0 Hz at 20 °C).

X-ray Crystallography

Crystals that were used in diffraction intensity measurements at low temperature were mounted on the tip of a quartz fiber and placed in a cold stream of nitrogen. Crystals that were used at room temperature were mounted and sealed in thin-walled glass capillaries under a nitrogen atmosphere. Diffraction measurements were made on an Enraf-Nonius CAD-4 automated diffractometer for compounds **2a**·$3CH_2Cl_2$, **2b**, and **3**·$3CH_2Cl_2$·$C_6H_5CH_3$, on a Syntex P3/F diffractometer for compound **2a**, and on an Enraf-Nonius FAST diffractometer with an area detector for compounds **2a**·$4C_6H_5CH_3$ and **2c**. All the diffractometers were equipped with graphite-monochromated Mo Kσ radiation. For the crystals on the CAD-4 and P3/F diffractometers, unit cells were determined by using search, center, index, and least-squares routines. The Laue classes and lattice dimensions were verified by axial oscillation photography. The intensity data were corrected for Lorentz and polarization effects and for anisotropic decay. Empirical absorption corrections based on ψ scans were also applied. For the crystals on the FAST diffractometer, a preliminary data collection was carried out to establish all parameters and an orientation matrix. Fifty reflections were used in indexing and 250 reflections in cell refinement. Axial images were obtained to determine the Laue groups and cell dimensions. No decay correction and absorption correction were applied.

(13) Hartmann, E.; Dehnicke, K.; Fenske, D.; Goesmann, H.; Baum, G. *Z. Naturforsch., B* **1989**, *44*, 1155.

(14) a = 9.595(1) Å, b = 19.566(3)Å, c = 15.049(1)Å, β = 98.50(1)°, V = 2794(1) Å^3, space group $P2_1/c$. The structure will be discussed in a later report.

Table 1. Crystal Data for Compounds **2a**·$3CH_2Cl_2$, **2a**, **2a**·$4C_6H_5CH_3$, **2b**, **2c**·2.43CH_3CN, and **3**·$3CH_2Cl_2$·$C_6H_5CH_3$

	2a·$3CH_2Cl_2$	**2a**	**2a**·$4C_6H_5CH_3$	**2b**	**2c**·2.43CH_3CN	**3**·$3CH_2Cl_2$·$C_6H_5CH_3$
empirical formula	$C_{75}H_{71}Cl_{24}P_3Zr_6$	$C_{72}H_{65}Cl_{18}P_3Zr_6$	$C_{100}H_{97}Cl_{18}P_3Zr_6$	$C_{36}H_{89}Cl_{18}N_3Zr_6$	$C_{28.87}H_{70.92}Cl_{18}N_{5.43}Zr_6$	$C_{82}H_{79}Cl_{23.19}I_{0.81}P_3Zr_6$
fw	2463.35	2208.57	2577.11	1749.52	1679.77	2629.79
crystal system	triclinic	tetragonal	triclinic	cubic	orthorhombic	monoclinic
space group	$P\bar{1}$	$I4_1/a$	$P\bar{1}$	$Im\bar{3}m$	*Pnma*	$P2_1/c$
a, Å	15.993(3)	33.196(2)	14.501(5)	15.093(3)	21.156(1)	19.786(5)
b, Å	22.237(3)	33.196(2)	26.630(9)	15.093(3)	24.584(3)	19.071(4)
c, Å	14.670(4)	15.236(2)	14.049(5)	15.093(3)	11.713(2)	27.397(5)
α, deg	95.31(1)	90	90.39(3)	90	90	90
β, deg	112.07(2)	90	94.19(3)	90	90	90.22(3)
γ, deg	82.06(2)	90	82.59(1)	90	90	90
V, Å^3	4784(2)	16790(3)	5365(3)	3438(1)	6092(1)	10337(4)
Z	2	8	2	2	4	4
d_{calcd}, g/cm^3	1.710	1.747	1.595	1.690	1.794	1.690
μ, cm^{-1}	13.89	13.88	10.98	16.03	18.04	15.11
instrument	CAD-4	P3/P	FAST	CAD-4	FAST	CAD-4
temp, °C	20	20	-60	-60	-100	20
$2\theta_{max}$, deg	45	45	50	60	50	46
no. of observns ($I > 2\sigma(I)$)	9573	2625	11345	329	4560	7775
no. of variables	1035	463	1174	39	309	1072
residuals: R1,[a] wR2[b]	0.037, 0.096	0.041, 0.064	0.069, 0.142	0.043, 0.109	0.086, 0.168	0.058, 0.123
quality-of-fit indicator[c]	1.070	0.912	1.055	1.024	1.260	1.072
max shift in final cycle	0.00	0.00	0.02	0.00	0.00	0.05
largest peak, e/Å^3	0.72(8)	0.6(2)	1.1(2)	0.53(9)	1.0(2)	1.0(2)
absorption correction	empirical	empirical	none	empirical	none	empirical

[a] $R1 = \sum||F_o| - |F_c||/\sum|F_o|$ (based on reflections with $F_o^2 > 2\sigma(F_o^2)$). [b] $wR2 = [\sum[w(F_o^2 - F_c^2)^2/\sum[w(F_o^2)^2]]^{1/2}$; $w = 1/[\sigma^2(F_o^2) + (0.095P)^2]$; $P = [\mathrm{Max}(F_o^2, 0) + 2F_c2]/3$ (also with $F_o^2 > 2\sigma(F_o2)$). [c] Quality-of-fit (on F^2) $= [\sum[w(F_o^2 - F_c^2)^2]/(N_{observns} - N_{params})]^{1/2}$.

Each structure was solved by a combination of direct methods using the SHELXS-86 program[15a] and least-squares refinement using SHELXL-93.[15b] Crystallographic data and results are listed in Table 1.

Compound **2a**·$3CH_2Cl_2$ crystallized in the triclinic crystal system. The space group $P\bar{1}$ (No. 2) was assumed and confirmed by successful solution and refinement of the structure. There are two independent cluster anions, $[Zr_6Cl_{18}H_5]^{3-}$, in the unit cell. In one of the CH_2Cl_2 solvent molecules, two Cl atoms were found to be disordered at three positions. In the other CH_2Cl_2 solvent molecule, every non-hydrogen atom was disordered at two positions. All non-hydrogen atoms, except the carbon atoms for the disordered CH_2Cl_2 solvent molecules, were refined with anisotropic thermal parameters. The positions of the hydrogen atoms on the phenyl rings were calculated by assuming idealized geometries, C−H = 0.93 Å. They were refined with fixed thermal parameters set at 1.2 × B_{eqv} of the corresponding carbon atoms.

Compound **2a** crystallized in the tetragonal crystal system. The space group $I4_1/a$ (No. 88) was identified uniquely from the systematic absences in the data. All non-hydrogen atoms were refined with anisotropic thermal parameters. The positions of the hydrogen atoms on the phenyl rings were calculated by assuming idealized geometries, C−H = 0.93 Å. They were refined with fixed thermal parameters set at 1.2 × B_{eqv} of the corresponding carbon atoms.

Compound **2a**·$4C_6H_5CH_3$ crystallized in the triclinic crystal system. The space group $P\bar{1}$ (No. 2) was assumed and confirmed by successful solution and refinement of the structure. There are also two independent cluster anions, $[Zr_6Cl_{18}H_5]^{3-}$, in the unit cell. All non-hydrogen atoms were refined with anisotropic thermal parameters. The positions of the hydrocarbon hydrogen atoms were calculated by assuming idealized geometries, C−H = 0.93 Å for phenyl groups and C−H = 0.97 Å for methyl groups. They were refined with fixed thermal parameters set at 1.2 × B_{eqv} and 1.5 × B_{eqv} of the corresponding carbon atoms, respectively.

Compound **2b** crystallized in the cubic crystal system. The space group $Im\bar{3}m$ (No.229) was assumed and confirmed by successful solution and refinement of the structure. The propyl groups in $[Pr_4N]^+$ were disordered at two positions. All non-hydrogen atoms were refined with anisotropic thermal parameters.

Compound **2c**·2.43CH_3CN crystallized in the orthorhombic crystal system. The space group *Pnma* (No. 62) was assumed and confirmed by successful solution and refinement of the structure. All non-hydrogen atoms were refined with anisotropic thermal parameters. The positions of the hydrogen atoms of the $[Et_4N]^+$ cations were calculated by assuming idealized geometries, C−H = 0.97 Å for methylene groups and C−H = 0.98 Å for methyl groups. They were refined with fixed thermal parameters set at 1.2 × B_{eqv} and 1.5 × B_{eqv} of the corresponding carbon atoms, respectively. The total number of MeCN solvate molecules was obtained from the result of refinement on their occupancies.

Compound **3**·$3CH_2Cl_2$·$C_6H_5CH_3$ crystallized in the monoclinic crystal system. The space group $P2_1/c$ (No. 14) was identified uniquely from the systematic absences in the data. There are two independent cluster anions, $[Zr_6Cl_{18-x}I_xH_5]^{3-}$, in the unit cell. The I atoms were refined with constraints of a fixed distance of Zr−I = 2.80(2) Å. All non-hydrogen atoms except those of the toluene solvent molecule were refined with anisotropic thermal parameters. The positions of hydrogen atoms in the $[Ph_4P]^+$ cations and CH_2Cl_2 solvent molecules were calculated by assuming idealized geometries, C−H = 0.93 Å for phenyl groups and C−H = 0.97 Å for methylene groups. They were refined with fixed thermal parameters set at 1.2 × B_{eqv} of the corresponding carbon atoms.

Results and Discussion

Reduction of $ZrCl_4$ with $HSnBu_3$ resulted in the formation of a brown solid, **1**. Although we have not been able to characterize brown solid **1** structurally, we have found that it is a good starting material for the preparation of zirconium cluster

(15) (a) Sheldrick, G. M. *SHELXS-86: Program for Crystal Structure Determination*; University of Cambridge: Cambridge, England, 1986. (b) Sheldrick, G. M. *SHELXL-93*: *Fortran-77 program for the refinement of crystal structures from diffraction data*; University of Göttingen: Göttingen, Germany, 1993.

(16) (a) Böttcher, F.; Simon, A.; Kremer, R. K.; Buchkremer-Hermanns, H.; Cockcroft, J. K. *Z. Anorg. Allg. Chem.* **1991**, *598*, 25. (b) Simon, A.; Böttcher, F.; Cockcroft, J. K. *Angew. Chem., Int. Ed. Engl.* **1991**, *30*,101.

(17) (a) Bezman, S. A.; Churchill, M. R.; Osborn, J. A.; Wormald, J. *J. Am. Chem. Soc.* **1971**, *93*, 2063. (b) Churchill, M. R.; Bezman, S. A.; Osborn, J. A.; Wormald, J. *Inorg. Chem.* **1972**, *11*, 1818. (c) Stevens, R. C.; Maclean, M. R.; Bau, R. *J. Am. Chem Soc.* **1989**, *111*, 3472. (d) Lemmen, T. H.; Folting, K.; Huffman, J. C.; Caulton, K. G. *J. Am. Chem.* **1985**, *107*, 7774.

(18) Shoer, L. I.; Gell, K. I.; Schwartz, J. *J. Organomet. Chem.* **1977**, *136*, C19.

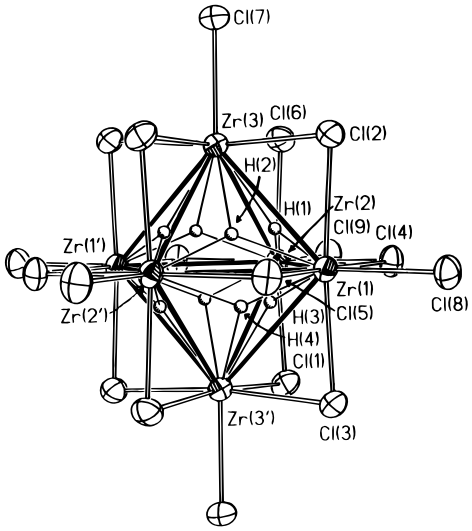

Figure 1. ORTEP diagram of $[Zr_6Cl_{18}H_5]^{3-}$ in $[Ph_4P]_3[Zr_6Cl_{18}H_5]\cdot 3CH_2Cl_2$ showing 30% probability thermal ellipsoids. The most likely positions for hydrogen atoms are shown.

Scheme 1

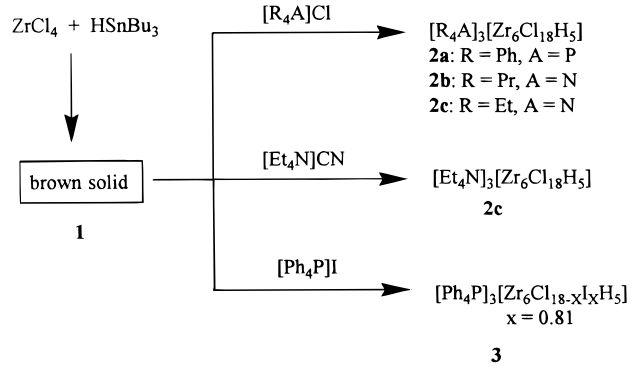

compounds.[9−12] Reaction of brown solid **1** with a phosphonium or ammonium chloride provides a direct method for synthesis of compounds containing $[Zr_6Cl_{18}H_5]^{3-}$ cluster anions, as shown in Scheme 1.

Addition of $[Ph_4P]Cl$ to brown solid **1** yielded $[Ph_4P]_3[Zr_6Cl_{18}H_5]$, **2a**. Compound **2a** crystallized in several forms with different types and numbers of solvent molecules, depending on the solvents used for crystallization. Compounds **2a**·$3CH_2Cl_2$ and **2a**·$4C_6H_5CH_3$ were isolated when a CH_2Cl_2−toluene solvent system was used for crystallization, and compound **2a** without solvent molecules was obtained when a CH_3CN−Et_2O−hexane solvent system was used.

Compound **2a**·$3CH_2Cl_2$ was characterized by X-ray single-crystal diffraction and ^1H NMR spectroscopy. An ORTEP diagram of the molecular structure of the cluster anion, $[Zr_6Cl_{18}H_5]^{3-}$, in compound **2a**·$3CH_2Cl_2$ is shown in Figure 1. Selected bond distances and angles are listed in Table 2. Six Zr atoms form an octahedron. There are 6 terminal and 12 bridging Cl atoms. The average Zr−Zr distance is 3.404(1) Å. The mean distance between a terminal Cl atom and a Zr atom, Zr−Cl_t, is shorter than that from a bridging Cl atom to a Zr atom, Zr−Cl_b, 2.479(2) Å *vs* 2.565(2) Å. The average Zr−Cl_b−Zr angle is 83.15(5)°.

The ^1H NMR spectrum of a single crystal of compound **2a**·$3CH_2Cl_2$ showed there are five cluster hydrogen atoms from an integration of the cluster hydrogen signal against the phenyl hydrogen signals. The cluster hydrogen signal appeared at −3.07 ppm as a slightly broad singlet ($\Delta\nu_{1/2}$= 1.83 Hz at 20 °C). No resolved coupling between cluster hydrogen atoms was observed. The ^1H NMR spectrum of a sample containing 50% $[Ph_4P]_3[Zr_6Cl_{18}D_5]$ and 50% $[Ph_4P]_4[Zr_6Cl_{18}H_4]$ also showed that, at least over a period of 1 week, there is no exchange of cluster hydrogen atoms between the cluster anions, $[Zr_6Cl_{18}D_5]^{3-}$ and $[Zr_6Cl_{18}H_4]^{4-}$. The ^1H NMR signal for the cluster hydrogen atoms in $[Ph_4P]_3[Zr_6Cl_{18}(H_{1/2}D_{1/2})_5]$ was noticeably broader, $\Delta\nu_{1/2}$ = 3.12 Hz at 20 °C. This might be due to the additional

Table 2. Selected Bond Lengths (Å) and Angles (deg) for **2a**·$3CH_2Cl_2$[a]

Zr(1)−Zr(2)′	3.403(1)	Zr(1)−Cl(3)	2.568(2)
Zr(1)−Zr(3)′	3.406(1)	Zr(2)−Cl(6)	2.555(2)
Zr(2)−Zr(3)′	3.397(1)	Zr(2)−Cl(4)	2.564(2)
Zr(2)−Zr(1)′	3.403(1)	Zr(2)−Cl(1)	2.568(2)
Zr(3)−Zr(2)′	3.397(1)	Zr(2)−Cl(5)′	2.573(2)
Zr(3)−Zr(1)′	3.406(1)	Zr(3)−Cl(1)′	2.555(2)
Zr(11)−Zr(12)	3.3986(9)	Zr(3)−Cl(6)	2.557(2)
Zr(11)−Zr(13)′	3.404(1)	Zr(3)−Cl(3)′	2.565(2)
Zr(11)−Zr(12)′	3.411(1)	Zr(3)−Cl(2)	2.572(2)
Zr(12)−Zr(13)′	3.394(1)	Zr(11)−Cl(16)	2.559(2)
Zr(12)−Zr(11)′	3.411(1)	Zr(11)−Cl(14)	2.562(2)
Zr(13)−Zr(12)′	3.394(1)	Zr(11)−Cl(12)	2.566(2)
Zr(13)−Zr(11)′	3.404(1)	Zr(11)−Cl(13)	2.566(2)
Zr(2)−Cl(9)	2.466(2)	Zr(12)−Cl(14)	2.552(2)
Zr(1)−Cl(8)	2.488(2)	Zr(12)−Cl(11)	2.553(2)
Zr(3)−Cl(7)	2.481(2)	Zr(12)−Cl(15)	2.567(2)
Zr(11)−Cl(18)	2.486(2)	Zr(12)−Cl(16)′	2.580(2)
Zr(12)−Cl(19)	2.475(2)	Zr(13)−Cl(11)	2.551(2)
Zr(13)−Cl(17)	2.487(2)	Zr(13)−Cl(12)	2.566(2)
Zr(1)−Cl(5)	2.556(2)	Zr(13)−Cl(15)′	2.566(2)
Zr(1)−Cl(4)	2.561(2)	Zr(13)−Cl(13)′	2.570(2)
Zr(1)−Cl(2)	2.563(2)		
Zr(2)′−Zr(1)−Zr(3)′	59.99(2)	Zr(12)−Zr(11)−Zr(12)′	89.80(2)
Zr(1)−Zr(2)−Zr(3)′	60.18(2)	Zr(11)−Zr(12)−Zr(11)′	90.20(2)
Zr(3)′−Zr(2)−Zr(1)′	60.18(2)	Zr(12)′−Zr(13)−Zr(12)	89.87(2)
Zr(2)′−Zr(3)−Zr(1)′	59.89(2)	Zr(3)′−Cl(1)−Zr(2)	83.08(5)
Zr(2)−Zr(1)−Zr(3)′	59.92(2)	Zr(1)−Cl(2)−Zr(3)	83.20(5)
Zr(2)−Zr(3)−Zr(1)′	59.96(2)	Zr(3)′−Cl(3)−Zr(1)	83.15(5)
Zr(12)−Zr(11)−Zr(13)′	59.86(2)	Zr(1)−Cl(4)−Zr(2)	83.01(5)
Zr(13)′−Zr(11)−Zr(12)′	60.07(2)	Zr(1)−Cl(5)−Zr(2)′	83.12(5)
Zr(13)′−Zr(12)−Zr(11)	60.15(2)	Zr(2)−Cl(6)−Zr(3)	83.49(5)
Zr(13)′−Zr(12)−Zr(11)′	60.20(2)	Zr(13)−Cl(11)−Zr(12)	83.89(5)
Zr(12)′−Zr(13)−Zr(11)′	59.99(2)	Zr(13)−Cl(12)−Zr(11)	83.38(5)
Zr(11)′−Zr(13)−Zr(12)	60.07(2)	Zr(11)−Cl(13)−Zr(13)′	83.03(5)
Zr(2)−Zr(1)−Zr(2)′	89.76(2)	Zr(12)−Cl(14)−Zr(11)	83.31(5)
Zr(1)−Zr(2)−Zr(1)′	90.24(2)	Zr(13)′−Cl(15)−Zr(12)	82.78(5)
Zr(2)′−Zr(3)−Zr(2)	89.72(3)	Zr(11)−Cl(16)−Zr(12)′	83.16(5)

[a] Numbers in parentheses are estimated standard deviations in the least significant digits.

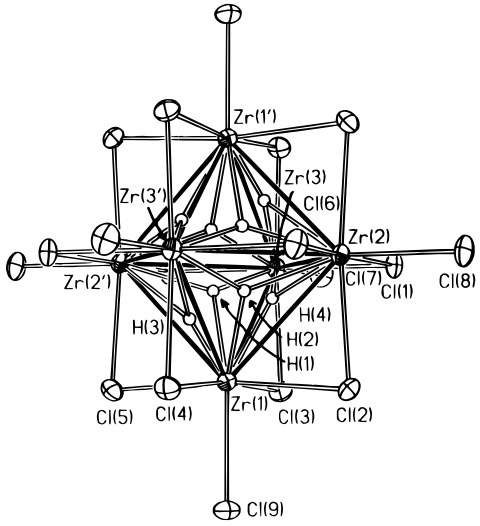

Figure 2. ORTEP diagram of $[Zr_6Cl_{18}H_5]^{3-}$ in $[Ph_4P]_3[Zr_6Cl_{18}H_5]\cdot 4C_6H_5CH_3$ showing 30% probability thermal ellipsoids. The most likely positions for hydrogen atoms are shown.

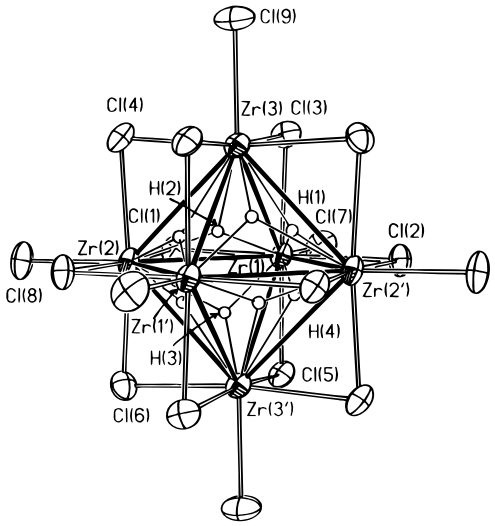

Figure 3. ORTEP diagram of $[Zr_6Cl_{18}H_5]^{3-}$ in $[Ph_4P]_3[Zr_6Cl_{18}H_5]$ showing 30% probability thermal ellipsoids. The most likely positions for hydrogen atoms are shown.

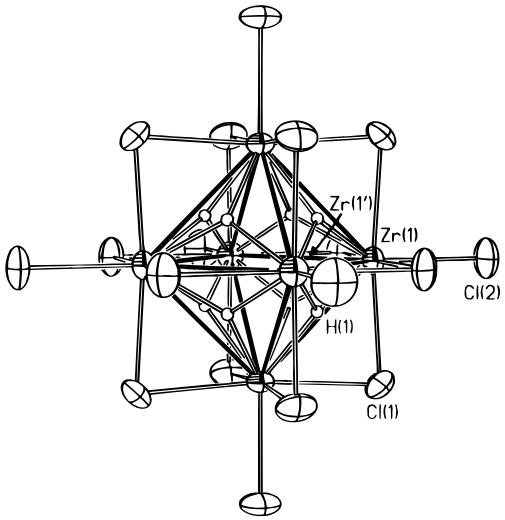

Figure 4. ORTEP diagram of $[Zr_6Cl_{18}H_5]^{3-}$ in $[Pr_4N]_3[Zr_6Cl_{18}H_5]$ showing 30% probability thermal ellipsoids. The most likely positions for hydrogen atoms are shown.

coupling from D atoms, which are heavier and thus less mobile than H atoms. An ^2H NMR study showed H−D coupling in the compound $[Ph_4P]_3[Zr_6Cl_{18}(H_{1/2}D_{1/2})_5]$. The deuterium signal was observed at −3.00 ppm ($CDHCl_2$ from solvent CH_2Cl_2 as reference). The width at half-height of the signal without decoupling H was 0.5 Hz broader than that with decoupling H, 2.7 Hz *vs* 2.2 Hz at 20 °C.

Compound **2a**·$4C_6H_5CH_3$ was isolated as a minor product along with compound **2a**·$3CH_2Cl_2$. It was also characterized by ^1H NMR and X-ray single-crystal diffraction. The structure of the cluster anion, $[Zr_6Cl_{18}H_5]^{3-}$, in compound **2a**·$4C_6H_5CH_3$ is almost identical with the structure of that in compound **2a**·$3CH_2Cl_2$. An ORTEP diagram of $[Zr_6Cl_{18}H_5]^{3-}$ in compound **2a**·$4C_6H_5CH_3$ is shown in Figure 2. Selected bond distances and angles are listed in Table 3. The mean Zr−Zr bond length is 3.413(1) Å, slightly longer than that in compound **2a**·$3CH_2Cl_2$, 3.404(1) Å. The $Zr-Cl_b$ and $Zr-Cl_t$ bond lengths are also slightly longer, 2.572(2) and 2.485(2) Å, respectively. The $Zr-Cl_b-Zr$ angle is almost the same, 83.17(6)°.

Crystals of compound **2a** without solvent molecules were obtained by using a CH_3CN−hexane−Et_2O solvent system. The chemical composition was confirmed by ^1H NMR. The structure of the cluster anion, $[Zr_6Cl_{18}H_5]^{3-}$, is shown in Figure 3. Selected bond distances and angles are listed in Table 4. The structure of the $[Zr_6Cl_{18}H_5]^{3-}$ anion in compound **2a** is virtually the same as those in the solvated compounds. The Zr−Zr, $Zr-Cl_b$, and $Zr-Cl_t$ bond lengths are 3.412(1), 2.569(2), and 2.483(2) Å, respectively. The $Zr-Cl_b-Zr$ angle is 83.25(7)°.

When the brown solid **1** was treated with $[Pr_4N]Cl$, the product was $[Pr_4N]_3[Zr_6Cl_{18}H_5]$, **2b**. An ^1H NMR study showed

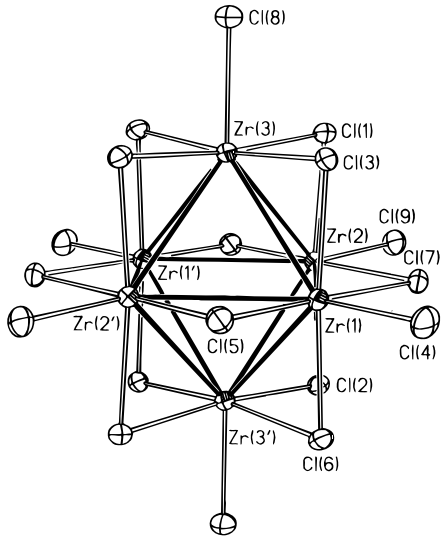

Figure 5. ORTEP diagram of $[Zr_6Cl_{18}]^{3-}$ in $[Et_4N]_3[Zr_6Cl_{18}H_5]$·$2.43CH_3CN$ showing 30% probability thermal ellipsoids.

Table 3. Selected Bond Lengths (Å) and Angles (deg) for **2a**·$4C_6H_5CH_3$[a]

Zr(1)−Zr(2)′	3.407(2)	Zr(2)−Cl(1)	2.571(2)
Zr(1)−Zr(3)′	3.413(2)	Zr(2)−Cl(2)	2.576(2)
Zr(1)−Zr(3)	3.414(2)	Zr(3)−Cl(7)	2.503(2)
Zr(2)−Zr(3)′	3.398(1)	Zr(3)−Cl(6)′	2.560(2)
Zr(2)−Zr(1)′	3.407(2)	Zr(3)−Cl(4)′	2.572(2)
Zr(3)−Zr(2)′	3.398(1)	Zr(3)−Cl(3)	2.580(2)
Zr(3)−Zr(1)′	3.413(2)	Zr(3)−Cl(1)	2.587(2)
Zr(11)−Zr(13)	3.407(2)	Zr(11)−Cl(18)	2.481(3)
Zr(11)−Zr(12)′	3.411(2)	Zr(11)−Cl(12)	2.569(3)
Zr(11)−Zr(12)	3.419(2)	Zr(11)−Cl(11)	2.570(3)
Zr(12)−Zr(13)′	3.405(2)	Zr(11)−Cl(15)	2.573(3)
Zr(12)−Zr(11)′	3.411(2)	Zr(11)−Cl(16)	2.578(3)
Zr(13)−Zr(12)′	3.405(2)	Zr(12)−Cl(13)	2.561(3)
Zr(13)−Zr(11)′	3.420(2)	Zr(12)−Cl(11)	2.570(2)
Zr(1)−Cl(9)	2.486(2)	Zr(12)−Cl(16)′	2.575(3)
Zr(1)−Cl(5)	2.564(2)	Zr(12)−Cl(14)	2.582(3)
Zr(1)−Cl(2)	2.567(2)	Zr(13)−Cl(19)	2.479(3)
Zr(1)−Cl(4)	2.573(2)	Zr(13)−Cl(13)	2.558(3)
Zr(1)−Cl(3)	2.582(2)	Zr(13)−Cl(12)′	2.571(3)
Zr(2)−Cl(8)	2.482(2)	Zr(13)−Cl(15)	2.572(2)
Zr(2)−Cl(6)	2.567(2)	Zr(13)−Cl(14)′	2.583(3)
Zr(2)−Cl(5)′	2.570(2)		

Zr(3)′−Zr(1)−Zr(3)	90.09(4)	Zr(13)′−Zr(12)−Zr(11)	60.16(3)
Zr(1)′−Zr(2)−Zr(1)	89.97(3)	Zr(12)′−Zr(13)−Zr(11)	60.10(3)
Zr(1)′−Zr(3)−Zr(1)	89.91(4)	Zr(12)′−Zr(13)−Zr(11)′	60.12(3)
Zr(12)′−Zr(11)−Zr(12)	89.99(4)	Zr(2)−Cl(1)−Zr(3)	83.39(7)
Zr(11)′−Zr(12)−Zr(11)	90.01(4)	Zr(1)−Cl(2)−Zr(2)	83.25(7)
Zr(11)−Zr(13)−Zr(11)′	90.07(4)	Zr(3)−Cl(3)−Zr(1)	82.80(7)
Zr(2)′−Zr(1)−Zr(3)′	60.41(3)	Zr(3)′−Cl(4)−Zr(1)	83.11(7)
Zr(2)′−Zr(1)−Zr(3)	59.75(3)	Zr(1)−Cl(5)−Zr(2)′	83.16(7)
Zr(3)′−Zr(2)−Zr(1)′	60.23(3)	Zr(3)′−Cl(6)−Zr(2)	83.01(7)
Zr(3)′−Zr(2)−Zr(1)	60.11(3)	Zr(11)−Cl(11)−Zr(12)	83.40(7)
Zr(2)′−Zr(3)−Zr(1)′	60.21(3)	Zr(11)−Cl(12)−Zr(13)′	83.44(8)
Zr(2)′−Zr(3)−Zr(1)	60.02(3)	Zr(13)−Cl(13)−Zr(12)	83.87(8)
Zr(13)−Zr(11)−Zr(12)′	59.93(3)	Zr(12)−Cl(14)−Zr(13)′	82.50(8)
Zr(13)−Zr(11)−Zr(12)	60.16(4)	Zr(13)−Cl(15)−Zr(11)	82.93(7)
Zr(13)′−Zr(12)−Zr(11)′	59.97(3)	Zr(12)′−Cl(16)−Zr(11)	82.89(8)

[a] Numbers in parentheses are estimated standard deviations in the least significant digits.

Table 4. Selected Bond Lengths (Å) and Angles (deg) for **2a**[a]

Zr(1)−Zr(3)′	3.407(1)	Zr(1)−Cl(5)	2.569(2)
Zr(1)−Zr(2)′	3.414(1)	Zr(1)−Cl(2)	2.579(2)
Zr(1)−Zr(3)	3.415(1)	Zr(1)−Cl(1)	2.581(2)
Zr(2)−Zr(3)	3.410(1)	Zr(2)−Cl(4)	2.550(2)
Zr(2)−Zr(1)′	3.414(1)	Zr(2)−Cl(1)	2.570(2)
Zr(2)−Zr(3)′	3.415(1)	Zr(2)−Cl(2)′	2.571(2)
Zr(3)−Zr(1)′	3.406(1)	Zr(2)−Cl(6)	2.574(3)
Zr(3)−Zr(2)′	3.415(1)	Zr(3)−Cl(4)	2.565(2)
Zr(1)−Cl(7)	2.473(2)	Zr(3)−Cl(3)	2.565(2)
Zr(2)−Cl(8)	2.497(2)	Zr(3)−Cl(5)′	2.568(2)
Zr(3)−Cl(9)	2.478(2)	Zr(3)−Cl(6)′	2.577(3)
Zr(1)−Cl(3)	2.564(2)		

Zr(3)′−Zr(1)−Zr(2)′	59.99(3)	Zr(2)−Zr(3)−Zr(2)′	90.18(3)
Zr(2)′−Zr(1)−Zr(3)	60.01(3)	Zr(2)−Cl(1)−Zr(1)	83.15(7)
Zr(3)−Zr(2)−Zr(1)′	59.89(3)	Zr(2)′−Cl(2)−Zr(1)	83.06(7)
Zr(1)′−Zr(2)−Zr(3)′	60.01(3)	Zr(1)−Cl(3)−Zr(3)	83.49(7)
Zr(1)′−Zr(3)−Zr(2)	60.12(3)	Zr(2)−Cl(4)−Zr(3)	83.62(7)
Zr(1)′−Zr(3)−Zr(2)′	60.14(3)	Zr(3)′−Cl(5)−Zr(1)	83.10(6)
Zr(3)′−Zr(1)−Zr(3)	89.88(3)	Zr(2)−Cl(6)−Zr(3)′	83.06(7)
Zr(3)−Zr(2)−Zr(3)′	89.82(3)		

[a] Numbers in parentheses are estimated standard deviations in the least significant digits.

Table 5. Selected Bond Lengths (Å) and Angles (deg)for **2b**[a]

Zr(1)−Zr(1)′	3.394(2)	Zr(1)−Cl(1)	2.557(2)
Zr(1)−Zr(1)′	3.394(2)	Zr(1)−Cl(1)′	2.557(2)
Zr(1)−Cl(2)	2.488(3)		

Zr(1)′−Zr(1)−Zr(1)′	60	Zr(1)−Cl(1)−Zr(1)′	83.16(8)
Zr(1)′−Zr(1)−Zr(1)′	90		

[a] Numbers in parentheses are estimated standard deviations in the least significant digits.

that it contains the same cluster anion, $[Zr_6Cl_{18}H_5]^{3-}$, as compounds **2a**·$2CH_2Cl_2$, **2a**·$4C_6H_5CH_3$, and **2a**. The number of cluster hydrogen atoms was again verified by ^{1}H NMR. The ORTEP diagram of $[Zr_6Cl_{18}H_5]^{3-}$ in compound **2b** is shown in Figure 4. Selected bond distances and angles are listed in Table 5. The cluster anion resides on a position of $m\bar{3}m$ symmetry, that is, perfect O_h symmetry. The average bond lengths of Zr−Zr and Zr−Cl_b are shorter than those found in compounds **2a**·$3CH_2Cl_2$, **2a**·$4C_6H_5CH_3$, and **2a**, 3.393(1) and 2.559(2) Å, respectively. The Zr−Cl_t length and Zr−Cl_b−Zr angle are almost the same, 2.484(4) Å and 83.08(6)°.

$[Et_4N]_3[Zr_6Cl_{18}H_5]$·$2.43CH_3CN$ (**2c**·$2.43CH_3CN$) was obtained from the reaction of brown solid **1** with [Et_4N]Cl. It was characterized by ^{1}H NMR and X-ray single-crystal diffraction. The structure of the cluster anion, $[Zr_6Cl_{18}]^{3-}$, is shown in Figure 5. Selected bond distances and angles are listed in Table 6. The structural features of $[Zr_6Cl_{18}H_5]^{3-}$ in compound **2c**·$2.43CH_3CN$ are virtually the same as those in compound **2a**·$4C_6H_5CH_3$. The bond lengths of Zr−Zr, Zr−Cl_b, and Zr−Cl_t are 3.413(1), 2.574(3), and 2.481(3) Å, respectively. The Zr−Cl_b−Zr angle is 83.07(8)°. The X-ray data here were not of sufficient quality to justify an attempt to locate cluster hydrogen atoms.

It is interesting to note that the addition of Cl^- is not necessary for the formation of $[Zr_6Cl_{18}H_5]^{3-}$ from brown solid **1**. An ^{1}H NMR study showed $[Zr_6Cl_{18}H_5]^{3-}$ was formed by dissolving brown solid **1** in CH_3CN. We have not been able to characterize the cation(s) in this solution by crystallization. There is some indication from the ^{1}H NMR spectrum that the cation(s) might contain butyl groups. However, $[Zr_6Cl_{18}H_5]^{3-}$ was not stable in this solution. It decomposed completely in 12 h. When [Et_4N]CN was introduced into the solution, the $[Zr_6Cl_{18}H_5]^{3-}$ cluster anion was stabilized and isolated as compound **2c**·$2.43CH_3CN$. In addition to providing $[Et_4N]^+$ cations, the [Et_4N]CN retarded the decomposition of $[Zr_6Cl_{18}H_5]^3$, but we do not know how.

Table 6. Selected Bond Lengths (Å) and Angles (deg) for **2c**·$2.43CH_3CN$[a]

Zr(1)−Zr(3)′	3.404(1)	Zr(1)−Cl(7)	2.579(3)
Zr(1)−Zr(2)′	3.411(1)	Zr(1)−Cl(6)	2.579(2)
Zr(1)−Zr(3)	3.421(1)	Zr(2)−Cl(2)	2.568(2)
Zr(1)−Zr(2)	3.425(1)	Zr(2)−Cl(1)	2.570(2)
Zr(2)−Zr(3)	3.402(1)	Zr(2)−Cl(7)	2.579(3)
Zr(3)−Zr(2)′	3.415(1)	Zr(2)−Cl(5)′	2.580(3)
Zr(1)−Cl(4)	2.481(3)	Zr(3)−Cl(3)	2.565(2)
Zr(2)−Cl(9)	2.469(3)	Zr(3)−Cl(1)	2.568(3)
Zr(3)−Cl(8)	2.493(3)	Zr(3)−Cl(6)′	2.578(3)
Zr(1)−Cl(3)	2.567(2)	Zr(3)−Cl(2)′	2.579(3)
Zr(1)−Cl(5)	2.573(3)		

Zr(3)′−Zr(1)−Zr(3)	89.67(3)	Zr(3)−Zr(2)−Zr(1)	60.14(3)
Zr(2)′−Zr(1)−Zr(2)	89.87(3)	Zr(3)′−Zr(2)−Zr(1)	59.69(3)
Zr(3)−Zr(2)−Zr(3)′	89.80(3)	Zr(2)−Zr(3)−Zr(1)′	60.16(3)
Zr(1)′−Zr(2)−Zr(1)	90.13(3)	Zr(1)′−Zr(3)−Zr(2)′	60.30(3)
Zr(2)−Zr(3)−Zr(2)′	90.20(3)	Zr(2)−Zr(3)−Zr(1)	60.26(3)
Zr(1)′−Zr(3)−Zr(1)	90.32(3)	Zr(2)′−Zr(3)−Zr(1)	59.87(3)
Zr(3)′−Zr(1)−Zr(2)′	59.89(3)	Zr(3)−Cl(1)−Zr(2)	82.93(7)
Zr(2)′−Zr(1)−Zr(3)	59.98(3)	Zr(2)−Cl(2)−Zr(3)′	83.14(7)
Zr(3)′−Zr(1)−Zr(2)	60.01(3)	Zr(3)−Cl(3)−Zr(1)	83.62(7)
Zr(3)−Zr(1)−Zr(2)	59.60(3)	Zr(1)−Cl(5)−Zr(2)′	82.91(8)
Zr(3)−Zr(2)−Zr(1)′	59.95(3)	Zr(3)′−Cl(6)−Zr(1)	82.61(7)
Zr(1)′−Zr(2)−Zr(3)′	60.15(3)	Zr(2)−Cl(7)−Zr(1)	83.24(7)

[a] Numbers in parentheses are estimated standard deviations in the least significant digits.

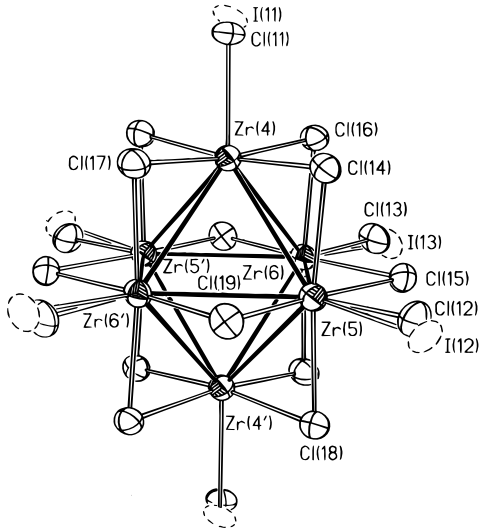

Figure 6. ORTEP diagram of $[Zr_6Cl_{18-x}I_x]^{3-}$ in $[Ph_4P]_3[Zr_6Cl_{18-x}I_x]$·$3CH_2Cl_2$·$C_6H_5CH_3$ (x = 0.81) showing 30% probability thermal ellipsoids.

$[Ph_4P]_3[Zr_6Cl_{18-x}I_xH_5]$ (x = 2.4) was obtained from the reaction of brown solid **1** with [Ph_4P]I. After recrystallization, the number of I atoms decreased to $x = 0.81$. The compositions were inferred from the refinement results of an X-ray single-crystal diffraction study. Evidently, a Cl atom is a better ligand than an I atom. It is possible that decomposition of a portion of $[Ph_4P]_3[Zr_6Cl_{18-x}I_xH_5]$ was the source of Cl atoms. $[Ph_4P]_3[Zr_6Cl_{18-x}I_xH_5]$·$3CH_2Cl_2$·$C_6H_5CH_3$ ($x = 0.81$) (**3**·$3CH_2Cl_2$·$C_6H_5CH_3$) was characterized by ^{1}H NMR and X-ray single-crystal diffraction. The signal for the cluster hydrogen atoms was also observed at −3.07 ppm. The structure of the cluster anion, $[Zr_6Cl_{18-x}I_x]^{3-}$, is shown in Figure 6. Selected bond distances and angles are listed in Table 7. Ignoring the I atoms, the structural features of $[Zr_6Cl_{18-x}I_x]^{3-}$ in compound **3**·$3CH_2Cl_2$·$C_6H_5CH_3$ are essentially the same as those in compound **2a**·$3CH_2Cl_2$. The bond lengths of Zr−Zr, Zr−Cl_b, and Zr−Cl_t are 3.404(2), 2.571(3), and 2.49(1) Å, respectively. The Zr−

Table 7. Selected Bond Lengths (Å) and Angles (deg) for **3**·$3CH_2Cl_2$·$C_6H_5CH_3$[a]

Zr(1)−Zr(3)	3.387(2)	Zr(1)−Cl(6)	2.585(3)
Zr(1)−Zr(3)′	3.395(2)	Zr(2)−Cl(4)′	2.559(3)
Zr(1)−Zr(2)	3.399(2)	Zr(2)−Cl(7)′	2.562(3)
Zr(1)−Zr(2)′	3.405(2)	Zr(2)−Cl(9)	2.565(3)
Zr(2)−Zr(3)	3.396(2)	Zr(2)−Cl(5)	2.573(3)
Zr(2)−Zr(3)′	3.405(2)	Zr(3)−Cl(8)	2.553(3)
Zr(2)−Zr(1)′	3.405(2)	Zr(3)−Cl(7)	2.564(3)
Zr(3)−Zr(1)′	3.395(2)	Zr(3)−Cl(6)′	2.566(3)
Zr(3)−Zr(2)′	3.405(2)	Zr(3)−Cl(5)	2.570(3)
Zr(4)−Zr(5)′	3.404(2)	Zr(4)−Cl(18)′	2.568(3)
Zr(4)−Zr(6)	3.404(2)	Zr(4)−Cl(14)	2.572(3)
Zr(4)−Zr(5)	3.408(2)	Zr(4)−Cl(16)	2.576(3)
Zr(4)−Zr(6)′	3.413(2)	Zr(4)−Cl(17)	2.581(3)
Zr(5)−Zr(6)	3.400(2)	Zr(5)−Cl(18)	2.573(3)
Zr(5)−Zr(4)′	3.404(2)	Zr(5)−Cl(15)	2.574(3)
Zr(5)−Zr(6)′	3.418(2)	Zr(5)−Cl(14)	2.576(3)
Zr(6)−Zr(4)′	3.413(2)	Zr(5)−Cl(19)	2.589(3)
Zr(6)−Zr(5)′	3.418(2)	Zr(6)−Cl(16)	2.574(3)
Zr(1)−Cl(1)	2.49(1)	Zr(6)−Cl(15)	2.575(3)
Zr(2)−Cl(2)	2.49(1)	Zr(6)−Cl(19)′	2.584(3)
Zr(3)−Cl(3)	2.484(3)	Zr(6)−Cl(17)′	2.587(3)
Zr(4)−Cl(11)	2.478(8)	Zr(1)−I(1)	2.79(2)
Zr(5)−Cl(12)	2.50(1)	Zr(2)−I(2)	2.81(1)
Zr(6)−Cl(13)	2.50(1)	Zr(4)−I(11)	2.78(2)
Zr(1)−Cl(8)	2.543(3)	Zr(5)−I(12)	2.80(1)
Zr(1)−Cl(4)	2.551(3)	Zr(6)−I(13)	2.83(1)
Zr(1)−Cl(9)	2.578(3)		
Zr(3)−Zr(1)−Zr(3)′	89.95(4)	Zr(6)−Zr(5)−Zr(6)′	90.08(4)
Zr(3)−Zr(1)−Zr(2)	60.05(3)	Zr(4)′−Zr(5)−Zr(6)′	59.86(4)
Zr(3)′−Zr(1)−Zr(2)	60.15(3)	Zr(4)−Zr(5)−Zr(6)′	59.99(3)
Zr(3)−Zr(1)−Zr(2)′	60.17(3)	Zr(5)−Zr(6)−Zr(4)	60.13(4)
Zr(3)′−Zr(1)−Zr(2)′	59.92(4)	Zr(5)−Zr(6)−Zr(4)′	59.95(3)
Zr(2)−Zr(1)−Zr(2)′	90.31(4)	Zr(4)−Zr(6)−Zr(4)′	89.90(4)
Zr(3)−Zr(2)−Zr(1)	59.80(3)	Zr(5)−Zr(6)−Zr(5)′	89.92(4)
Zr(3)−Zr(2)−Zr(3)′	89.64(4)	Zr(4)−Zr(6)−Zr(5)′	59.86(3)
Zr(1)−Zr(2)−Zr(3)′	59.87(3)	Zr(4)′−Zr(6)−Zr(5)′	59.86(4)
Zr(3)−Zr(2)−Zr(1)′	59.90(4)	Zr(1)−Cl(4)−Zr(2)′	83.56(9)
Zr(1)−Zr(2)−Zr(1)′	89.69(4)	Zr(3)−Cl(5)−Zr(2)	82.64(9)
Zr(3)′−Zr(2)−Zr(1)′	59.66(3)	Zr(3)′−Cl(6)−Zr(1)	82.46(9)
Zr(1)−Zr(3)−Zr(1)′	90.05(4)	Zr(2)′−Cl(7)−Zr(3)	83.24(9)
Zr(1)−Zr(3)−Zr(2)	60.14(3)	Zr(1)−Cl(8)−Zr(3)	83.32(9)
Zr(1)′−Zr(3)−Zr(2)	60.18(4)	Zr(2)−Cl(9)−Zr(1)	82.74(9)
Zr(1)′−Zr(3)−Zr(2)′	59.98(3)	Zr(4)−Cl(14)−Zr(5)	82.92(9)
Zr(2)−Zr(3)−Zr(2)′	90.36(4)	Zr(5)−Cl(15)−Zr(6)	82.63(9)
Zr(5)′−Zr(4)−Zr(6)	60.28(3)	Zr(6)−Cl(16)−Zr(4)	82.75(9)
Zr(5)′−Zr(4)−Zr(5)	90.02(4)	Zr(4)−Cl(17)−Zr(6)′	82.65(9)
Zr(6)−Zr(4)−Zr(5)	59.87(4)	Zr(4)′−Cl(18)−Zr(5)	82.91(9)
Zr(5)′−Zr(4)−Zr(6)′	59.83(3)	Zr(6)′−Cl(19)−Zr(5)	82.72(9)
Zr(6)−Zr(4)−Zr(6)′	90.10(4)	Cl(13)−Zr(6)−I(13)	4(1)
Zr(5)−Zr(4)−Zr(6)′	60.15(3)	Cl(1)−Zr(1)−I(1)	4(3)
Zr(6)−Zr(5)−Zr(4)′	60.21(3)	Cl(2)−Zr(2)−I(2)	7.5(6)
Zr(6)−Zr(5)−Zr(4)	60.00(4)	Cl(11)−Zr(4)−I(11)	3(1)
Zr(4)′−Zr(5)−Zr(4)	89.98(4)	Cl(12)−Zr(5)−I(12)	5.8(9)

[a] Numbers in parentheses are estimated standard deviations in the least significant digits.

Cl_b−Zr angle is 82.88(9)°. Iodine atoms are found only at the terminal positions, Zr−I = 2.80(2) Å.

Conclusions

Preparative Procedures. Compounds containing the $[Zr_6Cl_{18}H_5]^{3-}$ cluster anion can be readily prepared from reduction of $ZrCl_4$ with $HSnBu_3$ followed by addition of ammonium or phosphonium chloride (Scheme 1). While the addition of Cl^- is not necessary for the formation of $[Zr_6Cl_{18}H_5]^{3-}$, the ammonium or phosphonium cations are essential for the stabilization and isolation of the cluster anion.

Metrical Parameters of the $[Zr_6Cl_{18}H_5]^{3-}$ Cluster. Table 8 summarizes the bond distances and angles for compounds **2a**·$3CH_2Cl_2$, **2a**·$4C_6H_5CH_3$, **2a**, **2b**, **2c**·$2.43CH_3CN$, and **3**·$3CH_2Cl_2$·$C_6H_5CH_3$, as well as $[Zr_6Cl_{14}(PR_3)_4H_4]$ (R = Me, Et, or Pr).[12] As in $[Zr_6Cl_{14}(PR_3)_4H_4]$, one of the most outstanding structural features of the compounds containing $[Zr_6Cl_{18}H_5]^{3-}$ cluster anions is that the cluster hydrogen atoms are distributed, probably due to rapid movement of the hydrogen atoms, over eight triangular faces of the octahedron. The average Zr−Zr distance in $[Zr_6Cl_{18}H_5]^{3-}$ is longer than those in $[Zr_6Cl_{14}(PR_3)_4H_4]$, 3.407(1) *vs* 3.359(2) Å, but the Zr−Cl_b bond lengths are close, 2.568(4) *vs* 2.562(3) Å. The Zr−Cl_t distance in $[Zr_6Cl_{18}H_5]^{3-}$ is slightly shorter than that in $[Zr_6Cl_{14}(PR_3)_4H_4]$, 2.484(4) *vs* 2.495(3) Å.

The Cluster Hydrogen Atom Locations. In the $[Zr_6Cl_{18}H_5]^{3-}$ anion, the number, namely, 5, of cluster hydrogen atoms has been established with a high degree of confidence by observation and integration of the ^1H NMR signals for each compound. The question that immediately arises is, *Where* are they? The same question arises concerning the $[Zr_6Cl_{14}H_4(PR_3)_4]$ molecules[11] and the $[Zr_6Cl_{18}H_4]^{4-}$ ions.[12] X-ray data *alone* cannot answer this question, but they can help when taken in the context of an analysis as to where the hydrogen atoms *might* be.

When we rule out having them bridging the Zr−Zr edges, which are already bridged by Cl atoms, and we recognize the impossibility of putting more than one (or, just possibly, two) inside the cluster, we are left with only one possibility: namely, at or very near the centers of the Zr_3 faces. This in turn raises the question of which faces. Here the X-ray data are of some help by being most consistent with the hypothesis that they partially occupy all eight faces, giving an average occupancy of $^5/_8$ on each.

In each compound for which the X-ray data were of very high quality (all but **2c**·2.43MeCN), sites of residual electron density were found at or near all the face centers. When treated as hydrogen atoms and refined so that the thermal displacement parameters of all eight were constrained to be equal and the total occupancy was required to be 5, these sites were all found to behave reasonably. Except for those of **2b**, where all

Table 8. Average Bond Distances (Å) and Angles (deg) for $[Zr_6Cl_{18}H_5]^{3-}$ and $[Zr_6Cl_{14}(PR_3)_4H_4]$[a]

	Zr−Zr	Zr−Cl_b	Zr−Cl_t	Zr−Cl_b−Zr	ref
$[Ph_4P]_3[Zr_6Cl_{18}H_5]$·$2CH_2Cl_2$·$C_6H_5CH_3$ (20 °C)	3.404(1)	2.565(2)	2.479(2)	83.15(5)	this work
$[Ph_4P]_3[Zr_6Cl_{18}H_5]$ (20 °C)	3.412(1)	2.569(2)	2.483(2)	83.25(7)	this work
$[Ph_4P]_3[Zr_6Cl_{18}H_5]$·$4C_6H_5CH_3$ (−60 °C)	3.413(1)	2.572(2)	2.485(2)	83.17(6)	this work
$[Pr_4N]_3[Zr_6Cl_{18}H_5]$ (−60 °C)	3.393(1)	2.559(2)	2.484(4)	83.08(6)	this work
$[Et_4N]_3[Zr_6Cl_{18}H_5]$·2.43MeCN (−100 °C)	3.413(1)	2.574(3)	2.481(3)	83.07(8)	this work
$[Ph_4P]_3[Zr_6Cl1_{8-x}I_xH_5]$·$3CH_2Cl_2$·$C_6H_5CH_3$ (x = 0.81) (20 °C)	3.404(2)	2.571(3)	2.49(1)	82.88(9)	this work
$[HP(t\text{-}Bu)_2Ph]_3$[Zr6Cl18H5]·$2CH_2Cl_2$·$2C_6H_6$ (−60 °C)	3.416(2)	2.577(4)	2.486(4)	83.2(1)	12
$[Zr_6Cl_{14}(PMe_3)_4H_4]$·$2CH_2Cl_2$ (−75 °C)	3.335(1)	2.562(2)	2.495(2)	81.29(6)	12
$[Zr_6Cl_{14}(PEt_3)_4H_4]$·$2CH_2Cl_2$ (−60 °C)	3.340(1)	2.555(3)	2.500(3)	81.64(8)	12
$[Zr_6Cl_{14}(PPr)_4H_4]$·$2.31C_6H_6$ (−60 °C)	3.350(2)	2.563(4)	2.491(4)	81.6(1)	12
average for $[Zr_6Cl_{18}H_5]^{3-}$	3.407(1)	2.568(4)	2.484(4)	83.10(9)	
average for $[Zr_6Cl_{14}(PR_3)_4H_4]$	3.359(2)	2.562(3)	2.495(3)	81.5(1)	

[a] Numbers in parentheses are estimated standard deviations in the least significant digits.

occupancies are required to be equal by crystallographic symmetry, the occupancies of individual faces varied from as low as 0.37 to as high as 1.00. The apparent location of the fractional hydrogen atom always remained close to the face center.

A further question then arises: why do the five hydrogen atoms appear to be distributed fractionally over all eight faces? One possibility is that while only a subset of the faces are occupied in each individual cluster, the clusters are randomly disordered in the crystal. However, a fluxional model, in which the five protons move rapidly from face to face, is also consistent with the structural data.

We prefer the dynamic model because of the NMR data. There is no way to place five hydrogen atoms on the eight triangular faces of the Zr_6 octahedron so that they are all equivalent, but if they move rapidly on the NMR time scale, the observation of only one relatively sharp ^1H NMR signal can be understood. Similarly, for the anions with a mixture of H and D atoms, both the ^1H NMR and ^2H NMR signals are best explained for by the dynamic model. Because of solubility problems at temperatures appreciably below room temperature, we have been unable to obtain any evidence directly supportive of the dynamic model. We have, however, shown that intermolecular scrambling of hydrogen atoms does not occur, leaving intramolecular scrambling as the only possible dynamic model.

Finally, we note that, in the $[Zr_6Cl_{18}H_5]^{3-}$ anions, as in the $[Zr_6Cl_{14}H_4(PR_3)_4]$ molecules, the number of hydrogen atoms is sufficient to bring the number of cluster-based electrons (CBE) to 14. This conclusion is reached by assuming, formally, that the hydrogen atoms contribute their electrons to the pool derived from the remaining zirconium electrons, namely, nine or ten in the $[Zr_6Cl_{18}H_5]^{3-}$ and $[Zr_6Cl_{14}H_4(PR_3)_4]$ units, respectively. The protons (again, formally) then go to the most favorable positions in the electron density distributed over the Zr_6 octahedron, namely, the centers of the triangular faces.

Acknowledgment. We thank the Robert A. Welch Foundation for support under Grant A-494.

Supporting Information Available: X-ray crystallographic files, in CIF format, are available on the Internet only. Access information is given on any current masthead page.

IC960173I